Title Page

Low carbon availability in paleosols nonlinearly attenuates temperature sensitivity of SOM decomposition

Running title: Q_{10} of SOM decomposition in paleosols

Authors: Jiao Su[a,b], Haiyang Zhang[c], Xingguo Han[a,b], Josep Peñuelas[d,e], Ekaterina Filimonenko[f], Yong Jiang[g], Yakov Kuzyakov[h,i], Cunzheng Wei[a,j*]

Author affiliations:

[a] State Key Laboratory of Vegetation and Environmental Change, Institute of Botany, Chinese Academy of Sciences, Beijing, China

[b] University of Chinese Academy of Sciences, Beijing, China

[c] Hawkesbury Institute for the Environment, Western Sydney University, Penrith, New South Wales, Australia

[d] CSIC, Global Ecology Unit CREAF-CSIC-UAB, Bellaterra, Barcelona, Catalonia, Spain

[e] CREAF, Cerdanyola del Vallès, Barcelona, Catalonia, Spain

[f] Institute of Environmental and Agricultural Biology (X-BIO), Tyumen State University, 625003

This article has been accepted for publication and undergone full peer review but has not been through the copyediting, typesetting, pagination and proofreading process, which may lead to differences between this version and the Version of Record. Please cite this article as doi: 10.1111/GCB.16183

Tyumen, Russia

[g] College of Life Sciences, Hebei University, Baoding, China

[h] Dept. of Soil Science of Temperate Ecosystems, Dept. of Agricultural Soil Science, University of Goettingen, Göttingen, Germany

[i] Peoples Friendship University of Russia (RUDN University), 117198 Moscow, Russia

[j] Department of Terrestrial Ecology, Netherlands Institute of Ecology (NIOO-KNAW), Wageningen, The Netherlands

*** Corresponding authors:**

Cunzheng Wei, State Key Laboratory of Vegetation and Environmental Change, Institute ofBotany, Chinese Academy of Sciences, Xiangshan, Beijing 100093, China. Tel.: +86 10 62836974, E-mail: weicunzheng@ibcas.ac.cn

Type of article: Primary research article

ORCID IDs:

Jiao Su: https://orcid.org/0000-0001-5877-1084

Haiyang Zhang: https://orcid.org/0000-0001-7951-0502

Xingguo Han: https://orcid.org/0000-0002-1836-975X

Josep Peñuelas: https://orcid.org/0000-0002-7215-0150

Yakov Kuzyakov: https://orcid.org/0000-0002-9863-8461

Ekaterina Filimonenko: https://orcid.org/0000-0002-8146-4514

Yong Jiang: https://orcid.org/0000-0001-7518-5810

Cunzheng Wei: https://orcid.org/0000-0001-9309-2722

Abstract

Temperature sensitivity (Q_{10}) of soil organic matter (SOM) decomposition is an important parameter in models of the global carbon (C) cycle. Previous studies have suggested that substrate quality controls the intrinsic Q_{10}, whereas environmental factors can impose large constraints. For example, physical protection of SOM and its association with minerals attenuate the apparent Q_{10} through reducing substrate availability and accessibility ([*S*]). The magnitude of this dampening effect, however, has never been quantified. We simulated theoretical Q_{10} changes across a wide range of [*S*] and found that the relationship between Q_{10} and the $\log_{10}$-transformed [*S*] followed a logistic rather than a linear function. Based on the unique Holocene paleosol chronosequence (7 soils from ca. 500 to 6900 years old), we demonstrated that the Q_{10} decreased nonlinearly with soil age up to 1150 years, beyond which Q_{10} remained stable. Hierarchical partitioning analysisindicated that an integrated C availability index, derived from principal component analysis of DOC content and parameters reflecting physical protection and mineral association, was the main explanatory variable for the nonlinear decrease of Q_{10} with soil age. Microbial inoculation and ^{13}C-labelled glucose addition showed that low C availability induced by physical protection and minerals association attenuated Q_{10} along the chronosequence. A separate soil incubation experiment indicated that Q_{10} increased exponentially with activation energy (E_a) in the modern soil, suggesting that SOM chemical complexity regulates Q_{10} only when C availability is high. In conclusion, organic matter availability strongly decreased with soil age, whereas Michelis-Menten kinetics defines the Q_{10} response depending on C availability, but Arrhenius equation describes theeffects of increasing substrate complexity.

Keywords: Paleosol, physical protection, mineral association, organic matter stability, carbon cycling, global warming

1. Introduction

Soils contain most of the carbon (C) in the terrestrial biosphere, at least twice as much as that in the atmosphere (Jobbagy & Jackson, 2000; Schlesinger & Andrews, 2000; Tarnocai et al., 2009). The decomposition of soil organic matter (SOM) is temperature dependent (Davidson & Janssens, 2006; IPCC, 2013). Therefore, an increase in SOM mineralization induced by global warming would exacerbate the future climate change (Crowther et al., 2016; Smith & Fang, 2010; Todd-Brown et al., 2014). The magnitude of the C–climate feedback, however, is still uncertain (Trumbore & Czimczik, 2008), partly due to inaccurate parameterizations of the Q_{10} - the temperature sensitivity of SOM decomposition rate with 10 °C temperature rise (Conant et al., 2011; Knorr et al., 2005; Trumbore & Czimczik, 2008). Identifying the underlying mechanisms regulating Q_{10}, especially for pools of persistent C with long residence times, is thus crucial for accurately forecasting the future feedbacks of SOM to climate change.

The quantification of Q_{10} for SOM is rather difficult since it is regulated by an array of biotic and abiotic factors. For instance, soil microbial biomass and community composition drastically influence Q_{10} values (Balser & Wixon, 2009; Karhu et al., 2014; Li et al., 2021; Qin et al., 2021; Wang et al., 2018, 2021). Similarly, abiotic factors (e.g. nutrient availability, soil texture) also exert great effects on the Q_{10} values (Ding et al., 2018; Liu et al., 2017). Theoretically, SOM decomposition has been described by a common set of principles of kinetic theory, which states that substrate (i.e., organic C) quality and availability ([S]) concurrently control the responses of SOM decomposition to warming (Davidson & Janssens, 2006; Davidson et al., 2006, 2012; Liu et al., 2022). For C quality, the Arrhenius kinetics predicts that C with more complex compoundswill have a higher Q_{10} ("C quality-temperature hypothesis") (Bosatta & Ågren, 1999; Conant etal., 2008a, 2008b; Wang et al., 2018). Carbon availability also exerts large influence on Q_{10}, as described by the Michaelis–Menten kinetics (Craine et al., 2010; Giardina & Ryan, 2000; Gillabel et al. 2010; Liu et al., 2022; Tang et al., 2017). The inaccessibility of soil C to microbes and enzymes due to aggregate protection, mineral associations, or spatial heterogeneity may lead to a strong substrate limitation at reaction microsites (Davidson & Janssens, 2006; Jia et al., 2020; Kaiser & Guggenberger, 2003; Schulten & Leinweber, 2000; Sollins et al., 1996). Thus, it is

essential to highlight the effects of C availability on Q_{10} (Dungait et al., 2012; Gershenson et al., 2009; Liu et al., 2021).

Increased C availability raises temperature response of SOM decomposition both theoretically and empirically (Davidson & Janssens, 2006; von Lützow & Kögel-Knabner, 2009; Pang et al., 2015; Li et al., 2020). A linear relationship was found between Q_{10} and C availability index by Gershenson et al. (2009) and Liu et al. (2021), while no relationships have been also revealed by several other studies (Craine et al, 2010; Thiessen et al., 2013).. These linear or non-relationships, however, could be artefacts, mainly due to the narrow range of [S] in the tested soils (Liu et al., 2022).

The effects of [S] on Q_{10} could be well described by Michaelis–Menten kinetics, in which the decomposition rate (R_s) is equal to:

$$R_s = \frac{V_{max} \times [S]}{K_m + [S]} \qquad (1)$$

where $V_{\max}$ is the maximum rate of enzymatic reaction at a given temperature and K_{m} is the Michaelis–Menten (half-saturation) constant. When [S] ≈ K_{m}, the Q_{10} of a substrate can be determined from [S] and the sensitivity of both $V_{\max}$ and K_{m} to temperature ($Q_{10}^{V\max}$, $Q_{10}^{K\mathrm{m}}$). When [S] >> K_{m}, however, K_{m} becomes insignificant, and the response of SOM decomposition to temperature primarily depends on the $Q_{10}^{V\max}$. Similarly, when [S] << K_{m}, K_{m} becomes more relevant, the influence of [S] decreases. The prominent influence of [S] on Q_{10} has been discussed (Davidson & Janssens, 2006; Davidson et al., 2006; Blagodatskaya et al., 2016), but the Q_{10} changes across a wide range of [S] values has rarely been heuristically discussed and never experimentally tested.

It is simple to find a range of soils covering a broad range of C availabilities [S]. However, natural soils from various locations may have the confounding effects of many biotic and abiotic factors, such as soil texture and pH, vegetation types as well as land use history. This will impede a distinction of the importance of these complex factors in regulating the relationship between Q_{10} and [S]. Therefore, to test a large range of [S] values in undisturbed soils and to evaluate the relationship between Q_{10} and [S], the chronosequence approach can be used. We solved these

constrains to evaluate the effects of C availability on the Q_{10} changes by using a unique Holocene paleosol chronosequence that includes seven soil layers (hereafter referred to as S0–S6). The paleosols were developed from the same parent material and were formed during warm and wet periods and were subsequently buried by deposits of aeolian loess from the same origin during cold and dry periods (Jin et al., 2004). The ^{14}C dating showed the ages of C in these paleosols from 507 ± 60 to 6,903 ± 75 years before present (a BP) (Jin et al., 2004). A continuous decomposition of buried SOM in the paleosol decreased the available C content and therefore, is an ideal natural gradient of [S] during extremely long-term (geological) "incubation" (Retallack, 2001). More importantly, pedogenic calcite that forms between the deposition layers reduces root penetration and water percolation (Guo et al., 2002; Zamanian et al., 2016). Additionally, the experimental site has very sparse vegetation and low precipitation, therefore the fresh C input into the buried SOM pools is negligible.

Using this unique paleosol chronosequence, we conducted a series of laboratory incubation experiments in combination with theoretical simulation (Fig. 1) to test our core hypothesis: C availability, rather than C quality and soil biota, determines the non-linearity of the temperature sensitivity of SOM decomposition. Specifically, we aimed to address three questions: 1) How does Q_{10} change with substrate concentration [S] as affected by K_m and Q_{10} of V_{max} and K_m ($Q_0{}^{V_{max}}$, $Q_{10}{}^{K_m}$) when adopting the Michaelis–Menten kinetics? 2) Can this Q_{10}-[S] relationship be experimentally tested using a Holocene paleosol chronosequence that originates at the same site of temperate grassland vegetation, but differs greatly in [S] with age? 3) Can we rule out the effects of microbial properties, chemical complexity of SOM, soil texture and other edaphic properties on Q_{10} through a manipulation experiment?

2. Materials and methods

2.1 Theoretical simulation

To illustrate how Q_{10} responds to changes in [S], Q_{10} was calculated as the ratio of respiration rate between high and low temperature ($Q_{10} = R_{T+10}/R_T$), where R represents $V_{max} \times [S]/(K_m + [S])$. $Q_{10}{}^{V_{max}}$ and $Q_{10}{}^{K_m}$ were used to represent the temperature sensitivity of V_{max} and K_m,

respectively. We assumed that [S] remains stable with temperature. To reveal the relationship between Q_{10} values and [S], we first assigned a $Q_{10}^{V_{max}}$ reference value of 2 (Davidson et al., 2006), two scenarios for K_m (K_m = 1 or 10), and two scenarios for $Q_{10}^{K_m}$ ($Q_{10}^{K_m}$ = 1.5 or 2.0). Notably, Q_{10} was considered as following:

$$Q_{10} = Q_{10}^{V_{max}} \times \frac{K_m + [S]}{Q_{10}^{K_m} \times K_m + [S]} \quad (2)$$

We compressed the x-axis by $\log_{10}$-transforming [S] to enable a clearer visualization of the relationship between Q_{10} and [S]. Otherwise, the small Q_{10} values would have been overwhelmed by the relatively large range of [S] values (ranging from 10^{-3} to 10^{5}, which is in arbitrary units) (Metcalf & Casey, 2016).

2.2 Empirical experiments

2.2.1 Site description and soil sampling

The investigated aeolian paleosols are located in Hunshandake Sand Land, Inner Mongolia (43°52′36.6″N, 116°5′34.1″E; Fig. S1), which consist of six aeolian sand layers overlapping with six sandy paleosol layers, only the top aeolian sand has been eroded (Jin et al., 2004). The soil at this site is classified as Haplic Calcisols and Calcic-Orthic Aridisol by the Food and Agriculture Organization of the United Nations (FAO) and the USA soil classification system, respectively. The mean annual precipitation is 350 mm, and the mean annual temperature is 1.7 °C. The soil chronosequence is exposed in an east-west-oriented valley, at a depth of about 3–4 m (Fig. S1). Four profiles of the paleosol as independent replicates were selected. These four soil profiles were 20-50 m apart. Within each profile, seven soil depth samples were selected to represent a desired age interval. The details of soil sampling depth are provided in Table S1.

First, we removed the exposed soil in each profile before sampling (perpendicularly excavating 1 m of soil), since the outer layer of exposed soils is frequently subjected to disturbances, such as wind erosion. Soil samples were collected at intervals of 5 cm from the surface to the bottom of each profile, approximately to a depth of 4 m. A total of 320 soil samples collected were then transferred to the laboratory, passed through a 2-mm sieve, and air-dried. The

magnetic susceptibility (MS2B, Bartington, UK) and the soil organic carbon (soil C hereafter) content were analyzed to locate the paleosol layers along the profile. The soil ages were extracted from Jin et al. (2004), who dated the ^{14}C age of the same paleosol chronosequence. We re-analyzed the magnetic susceptibility and the soil C content in the soils of the chronosequence (Fig. S2). Our results matched with the data from Jin et al. (2004) exactly, enabling us to identify atotal of 7 paleosol layers from the top to the bottom, referred to as S0, S1, S2, S3, S4, S5, and S6, respectively (Fig. S1b, Table S1). The ^{14}C ages of S0 to S6 paleosols were 507 ± 60, 1,154 ± 65, 3,003 ± 46, 4,120 ± 51, 4,826 ± 85, 5,332 ± 74, and 6,903 ± 75 a BP, respectively. For simplicity, we will refer these ages in the text and Figures as: 500 1150, 3000, 4100, 4800, 5300 and 6900 a BP.

Second, after identifying the 7 paleosol layers, we recollected the 28 paleosol samples (4 profiles × 7 layers). All paleosol samples were sieved through a 2-mm mesh, and the visible roots and litter residues were manually removed from S0. The sieved samples were then immediately transferred to the laboratory and each divided into three subsamples. One subsample of the fresh paleosol was stored at 4 °C and analyzed to determine the contents of microbial biomass C (MBC). The second subsample was stored at −20 °C to determine the properties of the microbial community, and the third subsample was air-dried to determine the physical and chemical soil properties and for later incubation.

2.2.2 Soil physico-chemical properties and microbial analyses

The pH of the air-dried soil was measured at a 1:2.5 (*w/v*) soil/water ratio with a pH electrode (PB-10, Sartorius, Germany). The soil texture was measured using a Mastersizer 2000 particle-size analyzer following the standard procedure (Malvern Instrument Ltd., Worcestershire, UK). The total C (TC) and N (TN) contents were determined using a Vario EL III elemental analyzer (Elementar, Germany); the inorganic C content was measured using a multi EA 4000 (Analytic Jena, Germany). The soil C content was then calculated by subtracting the inorganic C content from the TC content. Soil base cations were extracted following the method as described by Ochoa-Hueso et al. (2014) and Lindsay (1978), and cation exchangeable capacity (CEC) was

calculated as the sum of eight extractable cations (K, Ca, Na, Mg, Fe, Mn, Cu, Zn). Total phosphorus (TP) was extracted using perchloric acid-sulfuric acid digestion and measured by colorimetric method with molybdenum blue (Table S2).

The MBC contents were analyzed using the chloroform fumigation method (Vance et al., 1987), and the composition of the microbial community was determined by measuring the contents of phospholipid fatty acids (PLFAs) (Bossio & Scow, 1998). The C and N contents of theextracts (DOC and DON contents) before and after the chloroform fumigation/extraction were measured using a multi N/C 3100 analyzer (Analytik Jena AG, Germany) to calculate MBC content.

2.2.3. Solid-state ^{13}C nuclear magnetic resonance (NMR) of SOM

Solid-state ^{13}C CPMAS (cross polarization with magic-angle spinning) NMR (nuclear magnetic resonance) were used to determine the chemical composition of SOM. First, an aliquot of 5 g soil was treated with 50 ml 10% hydrofluoric acid (HF) for seven times, then was rinsed with deionized water until a neutral pH, and frozen and lyophilized at −80 °C for 4 days (Li et al., 2017). The HF-treated samples (about 100 mg) were analyzed using Bruker Advance III 400 spectrometer equipped with a 7-mm CPMAS detector at a frequency of 100 MHz and a spin rateof 10,000 Hz. The peak proportion of each type of C to the total signal intensity was calculated using MestreNova 6.1.0 (Mestrelab Research S.L., Santiago de Compostela, Galicia, Spain). All spectra were grouped into seven categories as described in previous studies (Bonanomi et al.,2013; Li et al., 2017): 0–45 ppm (alkyl C), 45–60 ppm (N-alkyl/methoxyl C), 60–90 ppm (O-alkylC), 90–110 ppm (di-O-alkyl/anomeric C), 110–140 ppm (aryl C), 140–160 ppm (O-aryl C), and 160–190 ppm (carboxyl C). Three indices of decomposition were calculated to define the stability of SOM (Bonanomi et al., 2013; Li et al., 2010, 2017): A/O-A (the ratio of alkyl C to O-alkyl C), CC/MC (the ratio of carbohydrate C to methoxyl C), HB/HI (the ratio of hydrophobic C to hydrophilic C).

2.2.4. Aggregate and particle size fractionation

Air-dried soil samples (50 g) were divided into three size classes (macroaggregates (250– 2,000 μm), microaggregates (53–250 μm), and clay-silt (0–53 μm)) by wet-sieving, and theamount of sand in the macro- and microaggregates was determined by weighing the material retained on a 53-μm sieve after dispersal with sodium hexametaphosphate (5 g L^{-1}) (Márquez etal., 2004; Six et al., 1998). The geometric mean diameter (GMD), which increased with the aggregation degree, was calculated to assess the physical protection of SOM (van Steenbergen et al., 1991). The GMD was calculated as follows:

$$\mathrm{GMD}\ (\mu\mathrm{m}) = \exp[\sum_{i=1}^{n} W_i \log(X_i) / \sum_{i=1}^{n} W_i] \qquad (3)$$

where *i* represents the aggregate size class, *n* is the number of aggregate size classes, X_i is the average diameter of each aggregate size class (X_1, 26.5 μm; X_2, 151.5 μm and X_3, 1125 μm), and Wi is the proportion of the total sample weight occurring in each aggregate size class after corrected for the sand-mass.

The combination of density and size approaches, which separates SOM into particulate(POM) and mineral-associated (MAOM) forms, was also adopted. In brief, bulk soil (20 g) was dispersed in a 100 ml sodium iodide (NaI) solution with a density of 1.85 g cm^{-3} and thenshattered by ultrasonication with an ultrasonic homogenizer at an energy input of 150 J ml^{-1} (Li et al., 2018). Thereafter, the soil was separated into light fraction (light POM hereafter) and heavy fraction using 1.85 g cm^{-3} NaI (triple time). The light POM fraction was collected using glass microfiber filters (GF-F, Whatman, UK), and the remaining NaI of light POM and heavy fraction was rinsed with deionized water. Then, the heavy fraction was sieved through a 53-μm sieve to separate the sand-sized (>53-μm, also called heavy POM fraction) and MAOA (<53-μm, clay+silt fraction) fraction. The recovery of soil weight was > 97.4%. After density and size fractionation, the weight and soil C content of the light POM, heavy POM and MAOM fractions were measured.The soil C content of the light POM and heavy POM fraction were added together to represent the soil C content in POM fraction.

2.2.5. Soil incubation and Q_{10} calculation

Four incubation experiments were set up in a logical way (Fig. 1):

Experiment 1 (Exp1). Air-dried soil (200 g) was placed into a 400-mL airtight jar, and the water-holding capacity (WHC) was adjusted to 60%. Each layer had four replicates. The samples were covered with porous film and pre-incubated at 15 °C for 10 days; then, they were incubated under varying temperatures to calculate Q_{10}. The incubation temperatures were set to range from 10 to 30 °C by a 5 °C step. The temperature was initially increased from 10 to 30 °C and subsequently decreased from 30 to 10 °C to resemble the diurnal temperature dynamics in the fieldand account for the possible inconsistency of microbial response with ascending and descending temperature. This incubation method under diurnally-varying temperatures has been discussed in details by Chen et al. (2010) and its advantages over the conventional approaches under constant temperatures have been described in several recent publications (Fang et al., 2005; Wang et al., 2016, 2018; Zhu & Cheng, 2011).

All jars were allowed to equilibrate for 3 h to stabilize the soil conditions after each change in temperature. Subsequently, the jars were sealed with rubber stoppers and flushed with CO_2-free air for 8 min to equalize the initial CO_2 concentration among the samples. We incubated the jars for different time intervals to obtain gas samples with sufficient accumulated CO_2 concentrations for chromatographic analysis, depending on the incubation temperature (25, 15, 12, 8 and 6 h for 10, 15, 20, 25 and 30 °C, respectively). Finally, 20 mL of headspace gas were collected from each jar using syringes and analyzed using gas chromatography (GC, Agilent 7890A, California, USA). Four empty bottles were also incubated as blanks, and the WHC of 60% was maintained by weighing the bottles and adding deionized water every 2 days. The respiration rate was calculated as follows:

$$R_S = \frac{C_V \times M \times P \times V}{R \times T \times W} \qquad (4)$$

where R_S is the respiration rate (mg C kg^{-1} soil day^{-1}), C_V is the CO_2 concentration of a sample that respired for one day (ppm), M is the molecular weight of C (12 μg C μmol^{-1} CO_2), P is the atmospheric pressure (1 atm), V is the headspace volume of the bottle (L), R is the ideal air constant (0.0820575 L atm °K $mole^{-1}$), T is the incubation temperature (K = 273.15 + T), and $W$is the dry weight of the sample.

A first-order exponential model (Eq. 5) was applied to the results of each sample to fit the change in CO_2 emission rates (R_s, mg C kg^{-1} soil day^{-1}) to the respective temperatures (T, °C) (Li et al., 2021). Parameters *a* and *b* were obtained from the fitted models; then, *b* was used to calculate Q_{10} through Eq. 6:

$$R_s = a \times e^{bT} \quad (5)$$

$$Q_{10} = e^{10b} \quad (6)$$

2.2.6 Three experiments to examine factors affecting Q_{10}

Experiment 2 (Exp2).The paleosols (200 g) with or without addition of 1 mL of fresh inoculum suspension were incubated at both 10 and 25 °C, according to the range of meangrowing season temperature. Inoculum suspension was prepared from topsoil adjacent to a typical grassland in Inner Mongolia, since it contained more MBC and DOC than paleosols (282 and 93μg g^{-1}, respectively), which also could rule out the effect of the initial amount of microbialbiomass on soil respiration. Gas samples were collected after 10 days of pre-incubation (on day 1, 4, 10) to measure the CO_2 emission rates. Q_{10} was calculated for each soil sample as the change in emission rate (*R*, mg C kg^{-1} soil day^{-1}) between the two incubation temperatures:

$$Q_{10} = \frac{R_{25}^{(\frac{10}{T_{25} - T_{10}})}}{R_{10}} \quad (7)$$

Experiment 3 (Exp3). To test whether C availability attenuated Q_{10} in paleosols, we conducted a ^{13}C-labelled glucose addition experiment. By calculating Q_{10} of ^{13}C-labelled glucose, we partitioned the C availability, chemical complexity or other soil properties affecting Q_{10}. Bottles with air-dried paleosol samples (150g) were pre-incubated at 15 °C at 30% of WHC for 10 days to activate the soil microorganisms. After that, ^{13}C-labelled glucose solution was added to the soils to reach 60% of WHC, and then incubated at 10 and 25 °C separately. The ^{13}C-labelled glucose (2 atom %, $\delta^{13}C$ = 825 ‰) was added at an amount of 8 mg glucose g^{-1} dry soil. This amount was sufficient to remove C limitation for microbial respiration induced by low substrate availability in soil and also could reach the maximum respiration rate (Cheng & Coleman, 1989; West & Sparling, 1986). Gas samples were collected following the same procedure as in Exp1.

The CO_2 concentration was measured using a GC; moreover, the $\delta^{13}C$ value of the respired CO_2 was analyzed by isotope ratio mass spectrometry (IRMS 20-22; SerCon, Crewe, UK). Subsequently, a two-pool isotope mixing model was used to estimate the contribution of sources. The respired CO_2 was divided into SOM- and glucose-derived components through the following mass-balance equations:

$$R_{som} + R_{glu} = R_{total} \quad (8)$$

$$(R_{som} \times \delta_{som}) + (R_{glu} \times \delta_{glu}) = R_{total} \times \delta_{total} \quad (9)$$

where R_{som}, R_{glu}, and R_{total} are the respiration rates for SOM, glucose, and the total respired CO_2 after glucose addition (mg C kg^{-1} soil day^{-1}); moreover, δ_{som}, δ_{glu} (825 ‰), and δ_{total} represents their respective isotopic values. Q_{10} was calculated for each soil sample using equation 6.

Experiment 4 (Exp4). An incubation experiment was conducted to explore how Q_{10} change with the duration of the incubation, using soils from the same chronosequence. Paleosol samples (200g) were pre-incubated at 15 °C for 10 days with 1 mL of fresh soil suspension to equilibrate the soil and warrant the minimized initial differences in soil biota. The same diurnally-varying temperature technique as described in Exp1 was adopted to measure the CO_2 emission rates on days 1, 4, 10, and 24, respectively, and to calculate the corresponding Q_{10}.

In addition, the activation energy (E_a; KJ mol^{-1}) depending on incubation period was measured by fitting the SOM decomposition rate to the Arrhenius equation as follows (Craine et al., 2010):

$$R_s = \mathrm{A} \times e^{-\frac{E_a}{R \times T}} \quad (10)$$

where R_s is SOM decomposition rate (mg C kg^{-1} soil day^{-1}), A is a fitted constant, R is the gas constant (8.314 J K^{-1} mol^{-1}), and T is temperature (°C). By taking the logarithm of both sides of the equation, E_a was calculated as the slope of the relationship between −1/RT and the natural logarithm of R_s.

2.3 Statistical analysis

The differences in MBC, microbial community composition (PLFA), and Q_{10} were compared using one-way analysis of variance (ANOVA). The means were compared based on Fisher's

protected least significant difference (LSD), and statistical significance was accepted at $\alpha = 0.05$. Afterward, two-way ANOVA was used to analyze the effects of incubation time and soil age on Q_{10}. A nonparametric test (the Kruskal–Wallis test) was used to detect the differences in the fungi to bacteria ratios (F:B) and in $Q_{10}^{glucose}$, as the data were not normally distributed.

To explore the primary factors that could be ascribed to explain the changes of Q_{10} values, we classified all measured variables into five groups, including C availability, microbial properties, soil texture, chemical complexity and other edaphic factors, based on their relevance to a specific group of variables. All variables and the corresponding groups are listed in Table S3. Considering the strong correlations among the factors within each group (except chemical complexity), principal component analysis (PCA) was conducted to generate multivariate functional indices to represent C availability, microbial biomass, soil texture and other edaphic factors, respectively.The first component (PC1), which explained 39% to 72% of the total variance for these four groups, was used for subsequent analysis of the relationship between Q_{10} and the C availability index and calculation of the relative importance of each group through the hierarchical partitioninganalysis. If an indicator has a negative loading, its opposite was used in the group to ensure a positive loading, and all indicators were standardized (Luo et al., 2019). A linear correlation analysis was performed to reveal the relationships between the C availability and Q_{10}. Relative importance of C availability, microbial variables, chemical complexity of SOM, soil texture and other edaphic factors on Q_{10} was quantified by adopting the hierarchical partitioning method usingthe 'rdacca.hp' function in the 'rdacca.hp' package (Lai et al., 2022). All the data analyses were performed using the R statistical software v4.0.3 (R Development Core Team, 2020) and SigmaPlot v12.5 (Systat Software, Inc. San Jose, USA) for Windows.

3. Results

3.1 Theoretic simulations of the relationship between [*S*] and Q_{10}

The relationship between Q_{10} and the $\log_{10}$-transformed [*S*] followed a logistic rather than a linear function (Fig. 2). Three critical points characterize the relationship between Q_{10} and [*S*]: the point of maximum acceleration of Q_{10} increase (P_1), the inflection point (P_i, corresponding to a

null acceleration of Q_{10}) of the sigmoid curve, and the maximum negative acceleration (P_2).

3.2. SOM composition and physical protection along the paleosol chronosequence

The average soil C content along the paleosol chronosequence ranged from 2.10 ± 0.30 to 6.61 ± 0.26 g kg^{-1}, with the highest content in S5 (Table S2). The soil C content was increased with magnetic susceptibility (R^2 = 0.61, p < 0.0001). The percentage of O-alkyl C, mostly representing plant-derived labile C, decreased linearly with the depth: from 25% in S0 to 16% in S6 (Table S4, Fig. 3a). The alkyl/O-alkyl ratio (A/O-A), which represents the degree of SOM decomposition, increased linearly with soil age (Fig. 3b). The carbohydrate C to methoxyl C (CC/MC) and hydrophobic C to hydrophilic C (HB/HI) ratios also showed that the chemical complexity of the SOM linearly increased with soil age (Fig. S3). GMD, which is widely used to represent the degree of physical protection, increased linearly with the soil age (Fig. 3c). The mass weight of light POM and heavy POM fractions decreased with soil age, while the mass weight of MAOM increased with soil age (Fig. S4). Organic C occluded in POM (OC-POM, the proportion of C in POM fraction) declined nonlinearly, while organic C in MAOM (OC-MAOM, the proportion of C in MAOM) increased nonlinearly with soil age up to 1150 years. For paleosols older than 1150 years, the proportion of C in both POM and MAOM remained stable (p < 0.0001, Fig. 3d).

3.3. Changes of temperature sensitivity along the chronosequence

Two incubation experiments (Exp1-2) were conducted to determine the changes of Q_{10} along the chronosequence. First, we incubated the soils with increasing age under diurnal temperature dynamics to determine Q_{10} in realistic conditions (Q_{10} was the average of two temperature cycles on day 1 and day 44). Notably, Q_{10} decreased nonlinearly as the soil age increased (Fig. 4a): Q_{10} was the highest in the topsoil (S0); then, it dropped in S1 (1150 a BP), but further decrease fromS1 to S6 was absent (p < 0.0001).

The hierarchical partitioning analysis showed that C availability was the most important driver of the Q_{10} changes along the chronosequence, which explained 68% of Q_{10} variance among

the five variable groups (Fig. 4c). The spearman correlational analysis indicated that soil N content, C:N, pH, and texture significantly affected Q_{10} (Fig. 4b). Their relative contribution to the Q_{10} variance, however, was low. Edaphic factors, microbial variables and chemical complexity only explained 7.4%, 4.8% and 5.9% of the total variance, respectively. The soil texture explained a large proportion of the total variance (14%) (Fig. 4c). Therefore, we chose this newly-generated C availability index and then revealed its relationship with Q_{10}. The Q_{10} nonlinearly increased withthe C availability (Fig. 4d).

The total microbial, bacterial and fungal biomass decreased nonlinearly with the soil age (Figs. S5a-c), but the F:B ratio remained stable (p = 0.58, Fig. S5d). The inoculation experiment (Exp2) demonstrated that the interactive effects between microbial inoculation and soil age on Q_{10} were insignificant (p = 0.69, Fig. 5a).

3.4 Temperature sensitivity for SOM and ^{13}C-glucose decomposition

Glucose addition increased Q_{10} values in all soils for 0.5 to 2.0 units. The Q_{10} after glucose addition was similar between all soils (except Q_{10} in S6) (Fig. 5c). $Q_{10}^{glucose}$ (Q_{10} of the added glucose) was also similar in all soils (p= 0.11, Fig. 5d).

3.5 Effects of incubation duration on temperature sensitivity of SOM decomposition

There was a divergent pattern of Q_{10} between S0 and older paleosols (Fig. 5b). Obviously, the Q_{10} of S0 increased with the incubation time, while this raise was absent for paleosols older than 1,150 years (Fig. 5b, Table S5). The activation energy (E_a) of SOM mineralization in S0 increased with incubation time. The E_a of SOM mineralization in older paleosols decreased or remained stable during the incubation (Fig. S6, Table S6).

4. Discussion

4.1 Theoretical simulation of the nonlinear relationship between substrate availability and temperature sensitivity of SOM decomposition

The theoretical simulation showed that [S] played an important role in determining the

apparent Q_{10} (Davidson and Janssens, 2006; Davidson et al., 2006). By assigning the parameters in the Michaelis–Menten equation, three critical points were identified (Fig. 2): First, a very wide range (several orders of magnitude) of [S] values should be considered to identify the three criticalpoints. Second, Q_{10} is mainly determined by $Q_{10}^{V\max}$ when the [S] value > P_2, other parameters ([S], $Q_{10}^{K\mathrm{m}}$, and K_{m}) become insignificant. Under such circumstances, the Q_{10} can be well described by the Arrhenius kinetic equation (Liu et al., 2022). Third, the role of $Q_{10}^{K\mathrm{m}}$ becomes more conspicuous when [S] < P_1. In this case, [S] and K_{m} play very trivial roles in affecting Q_{10}. Fourth, $Q_{10}^{V\max}$, $Q_{10}^{K\mathrm{m}}$, K_{m}, and [S]$_0$ concurrently control Q_{10} when [S] falls between P_1 and P_2. In contrast to real Q_{10} described by Arrhenius law, the apparent Q_{10}, which reflects substrate availability and is described by Michaelis–Menten equation, decreased linearly with declining C availability (Gershenson et al., 2009; Li et al., 2020). Other studies demonstrated that Q_{10} is independent on soil depth (Briones et al., 2021; Fang et al., 2005; Hicks Pries et al., 2017). These findings, however, could result from the narrow range of [S] in the soils they tested.

4.2 Experimental evidence for the nonlinear attenuation of C availability on temperature sensitivity of SOM decomposition

The soil C content was increased with magnetic susceptibility ($R^2 = 0.61$, $p < 0.0001$). Higher magnetic susceptibility is related to greater enrichment of magnetic minerals, and high climate humidity (An et al., 1991; Jin et al., 2004; Zhou et al., 1990). During the humid periods, more vigorous vegetation growth and SOM accumulation is expected. A/O-A ratio, which represented the extent of SOM decomposition, increased linearly along the soil age (Fig. 3b). The buried SOMis experiencing continual (but very slow) decomposition, resulting in an increase of the SOM chemical complexity along the soil age. Continual decomposition of buried SOM in paleosols is common and could lead to C losses over 90% (Retallack, 2001).

Organic C protection indicated by GMD and the proportion of OC-MAOM tended to increase along the soil age (Figs. 2c, d). Such physical protection and organo-mineral associations prevented microorganisms and enzymes from contacting the substrates (Gentsch et al., 2018; Hassink & Whitmore, 1997; Lavallee et al., 2020; Mikutta et al., 2006; Six et al., 2002).

Independent of the absolute soil C content, the greater organic C association with a fine fraction decreases temperature sensitivity of SOM decomposition (Zimmermann et al., 2010) due to the inaccessibility of physically protected and mineral associated C for microbial organisms and enzymes (Qin et al., 2019, 2021). It has been further verified by the decreased C availability with soil age (Fig. S7).

The first incubation experiment (Exp1) demonstrated that Q_{10} decreased nonlinearly along the chronosequence. The hierarchical partitioning analysis further confirmed that C availability, rather than soil texture (proportion of sand, clay and silt fractions), microbial properties (MBC, fungi and bacteria PLFAs and F: B ratio), chemical complexity of SOM and other edaphic factors, contributes most to the Q_{10} change along the chronosequence (Fig. 4c).

Organic C occluded in POM (OC-POM) was mostly plant-derived and unprotected C, which is available for decomposition. The OC-MAOM is associated with clay minerals or iron oxides, strongly reduces exoenzymatic decomposition (Cotrufo et al., 2019; Lugato et al., 2021). The attenuating effect of the physical protection and mineral association of soil C on Q_{10} is especially common in subsoils (Gershenson et al., 2009; Gillabel et al., 2010; Qin et al., 2019). The physical protection and mineral associations reduce the accessibility of microbes and enzymes to soil C (Hassink & Whitmore, 1997; Mikutta et al., 2006, Wang et al., 2017, 2018), whereas the microbial abundance and enzyme activities are very low in subsoil (Loeppmann et al., 2016; Maharjan et al., 2017; Sheng et al., 2015). Our results confirmed that decreases in C availability due to physical protection and mineral associations explain the nonlinear decrease of Q_{10} along the chronosequence (Fig. 4c). The exponential increase of Q_{10} with C availability (new-extracted multivariate functional index) coincides well with our simulation results (Fig. 4d), but falls at points below P_2.

The Q_{10} nonlinearly decreased with soil age, even when fresh inoculum was added to narrow the differences in microflora along the chronosequence. The lower Q_{10} of inoculated soils was due to an exacerbated C limitation at a higher abundance and activity of microorganisms after inoculation (Craine et al., 2010). The nonlinear decrease of Q_{10} along the soil age disappeared and all Q_{10} values increased after the relief of C limitation by adding 8 mg g^{-1} glucose (Fig. 5c).

Addition of labile C would increases the Q_{10} (Liu et al., 2021; Pang et al., 2015; Xu et al., 2019), that agrees with our theoretical simulations when [*S*] exceeds the critical point P_2 (Fig. 2).

To further test the effects of C availability on Q_{10}, we calculated the Q_{10} of the added ^{13}C-labelled glucose ($Q_{10}^{glucose}$). The addition of ^{13}C-labelled glucose allowed the elimination of differences in quality (all received the same C source) and physical protection and mineral association (the added glucose is not protected and is not adsorbed to clay minerals, Kuzyakov and Jones, 2006) along the soil age. The $Q_{10}^{glucose}$ remained stable along the soil age (p = 0.11, Fig. 5d), suggesting that other soil biotic (microbial properties and activities) and abiotic factors (soil texture and nutrient availability) have no effects on the Q_{10} of glucose decomposition. Rather, low C availability induced by physical protection and mineral association is the main factor accounting for the nonlinearly attenuated Q_{10} along soil age, which is consistent with the general conclusion drawn from the ^{13}C-labelled straw addition experiments (Gillabel et al., 2010).

Furthermore, both Q_{10} and E_a increased during the experiment only in the topsoil, which has more labile C and lower effects of physical protection and mineral associated C compared to the buried soils (Conant et al., 2008b; Li et al., 2018) (Fig. S4). This Q_{10} and E_a increase is directly connected with the exhausting of labile C during the incubation, and suggests that the C quality is the main factor responsible for the Q_{10} in the topsoil (Fig. 6d, p <0.001). This coincides well with previous studies about increasing of Q_{10} with prolonged incubation, which is well explained by the Arrhenius equation (Conant et al., 2008b). During the incubation, the lability of the remaining SOM decreases as labile C was depleted, which resulted in an increase of E_a and Q_{10} in the topsoil. However, the Q_{10} in soils older than 1,150 years did not change with incubation time, suggesting that they are more constrained by low [*S*] (Gentsch et al., 2018; Gershenson et al., 2009; Gillabel et al., 2010; Qin et al., 2019).

Our main findings are summarized in Fig. 6. Two functions describe the relationships between Q_{10} and [*S*]: 1) based on Michaelis–Menten Equation (Fig. 6a) and 2) between Q_{10} andthe chemical complexity by the activation energy (E_a) of SOM based on Arrhenius-Equation (Fig. 6b). Based on soils directly collected from the field (Exp1), we found that Q_{10} was very low and independent on age for soils older than 1,000 years (Fig. 6c). This was mainly because the amount

of available C in these paleosols was lower than the characteristic point of P_1 (Fig. 2). The Q_{10} was much higher in the young topsoil, which fell in between P_1 and P_2. When glucose was added to provide sufficient available C, the Q_{10} value raised to the values that could be arbitrarily placed somewhere beyond P_2 (Fig. 6c). This pattern was described well by the Michaelis–Menten kinetics (Fig. 6a). The Q_{10} increased with E_a in the topsoil, but remained constant or evendecreased slightly for old soils (Fig. 6d), indicating that the quality (the chemical complexity of SOM) rather than the C availability exerted the strongest control on Q_{10} in the topsoil. Apparently,the Arrhenius equation clearly described the Q_{10} trend in the topsoil (Figs. 6b, 6d), while the Michaelis–Menten kinetics did so only in soils older than 1,150 years (Figs. 6a, 6c). To date, thisis the first theoretically based experimental study showing the nonlinear attenuating effect of C availability on Q_{10}. The use of a unique paleosol chronosequence reconciled the controversies about the application of the Arrhenius equations and the Michaelis–Menten kinetics to assess Q_{10} values of SOM decomposition.

5. Conclusions

Our theoretical simulation and experimental results showed that Q_{10} nonlinearly decreased with decreasing C availability, which could be ascribed to the increased physical protection and mineral association of SOM along a paleosol chronosequence ranging from 500 to 6900 years.The chemical complexity of SOM also regulates Q_{10} but only in soils having relatively high C availability (younger than 1150 years). The prevailing controversies over the relationship between Q_{10} and [S] might have arisen from the fact that the range of C availability in previously investigated soils was too narrow to encompass the three critical points of substrate availability [S](see theoretical simulations: Fig. 2, Fig. 6). The determination of C availability index, which integrates DOC, distribution of C in POM and MAOM fractions, and the physical protection, are recommended in place of a simple soil categorization for top- vs. subsoils and new vs. old soils to quantify the temperature sensitivity of SOM decomposition. Biogeochemical models of the C– climate feedbacks should consider not only the Arrhenius equations but also the Michaelis–Menten kinetics for more accurate forecast of the responses of soil C to global warming.

Acknowledgements

We are grateful to Shiling Yang for his helps for the locating and identifying the paleosol chronosequence. We also appreciate Professor Elise Pendall for her constructive comments on an early version of this manuscript. This work was financially supported by the Fund of the National Natural Science Foundation of China (32171601), and the National Key Research and Development Program of China (2016YFC0500700, 2017YFA0604802). J.P. acknowledges funding provided by the Spanish government project PID2019-110521GB-I00, the Catalan government project SGR2017-1005, and the Fundación Ramón Areces grant ELEMENTAL-CLIMATE. We thank for the support by the RUDN University Strategic Academic Leadership Program, the West-Siberian Interregional Science and Education Center's (project No. 89-DON 1), and Stability and Functions of Soil Carbon in Agroecosystems of Russia (CarboRus, 075-15-2021-610).

Declaration of competing interest

The authors declare no competing interests.

Statement of authorship

X.H. and C.W. developed the theoretical consideration and planned the study, while J.S. and C.W. performed the research. J.S., C.W., Y.J. and H.Z. were responsible for the sample collection and laboratory analyses. J.S., C.W. and Y.K. wrote the manuscript, and all authors contributed to reviewing the analyses and the text.

Data availability statement

The data supporting the findings of this study are available in Dryad at https://doi.org/10.5061/dryad.ns1rn8pw0.

References:

An, Z. H., Kukla, G. J., Porter, S. C., & Xiao, J. L. (1991). Magnetic susceptibility evidence of monsoon variation on the Loess Plateau of central China during the last 130,000 years. *Quaternary Research, 36*(1), 29-36. https://doi.org/10.1016/0033-5894(91)90015-w

Balser, T. C., & Wixon, D. L. (2009). Investigating biological control over soil carbon temperature sensitivity. *Global Change Biology, 15*(12), 2935-2949. https://doi.org/10.1111/j.1365-2486.2009.01946.x

Blagodatskaya E., Blagodatsky S., Khomyakov N., Myachina O., Kuzyakov Y. (2016). Temperature sensitivity and enzymatic mechanisms of soil organic matter decomposition along an altitudinal gradient on Mount Kilimanjaro. *Scientific Reports*, *6*(1), 22240. https://doi.org/10.1038/srep22240

Bonanomi, G., Incerti, G., Giannino, F., Mingo, A., Lanzotti, V., & Mazzoleni, S. (2013). Litter quality assessed by solid state ^{13}C NMR spectroscopy predicts decay rate better than C/N and Lignin/N ratios. *Soil Biology and Biochemistry, 56*, 40-48. https://doi.org/10.1016/j.soilbio.2012.03.003

Bosatta, E., & Ågren, G. I. (1999). Soil organic matter quality interpreted thermodynamically. *Soil Biology and Biochemistry*, *31*(13), 1889-1891. https://doi.org/10.1016/S0038-0717(99)00105-4

Bossio, D. A., & Scow, K. M. (1998). Impacts of carbon and flooding on soil microbial communities: phospholipid fatty acid profiles and substrate utilization patterns. *Microbial Ecology, 35*(3), 265-278. https://doi.org/10.1007/s002489900082

Briones, M.J. , Garnett, M.H., & Ineson, P. (2021). No evidence for increased loss of old carbon in a temperate organic soil after 13 years of simulated climatic warming despite increased CO_2 emissions. *Global Change Biology*, *27*(9), 1836-1847. . https://doi.org/10.1111/gcb.15540.

Chen, X., Tang, J., Jiang, L., Li, B., Chen, J., & Fang, C. (2010). Evaluating the impacts of incubation procedures on estimated Q_{10} values of soil respiration. *Soil Biology and Biochemistry, 42*(12), 2282-2288. https://doi.org/10.1016/j.soilbio.2010.08.030

Cheng, W. X., & Coleman, D. C. (1989). A simple method for measuring CO_2 in a continuous air-flow system – modifications to the substrate-induced respiration technique. *Soil Biology and Biochemistry, 21*(3), 385-388. https://doi.org/10.1016/0038-0717(89)90148-X

Conant, R. T., Drijber, R. A., Haddix, M. L., Parton, W. J., Paul, E. A., Plante, A. F., . . . Steinweg, J. M. (2008a). Sensitivity of organic matter decomposition to warming varies with its quality. *Global Change Biology, 14*(4), 868-877. https://doi.org/10.1111/j.1365-2486.2008.01541.x

Conant, R. T., Ryan, M. G., Ågren, G. I., Birge, H. E., Davidson, E. A., Eliasson, P. E., . . . Bradford, M. A. (2011). Temperature and soil organic matter decomposition rates - synthesis of current knowledge and a way forward. *Global Change Biology, 17*(11), 3392-3404. https://doi.org/10.1111/j.1365-2486.2011.02496.x

Conant, R. T., Steinweg, J. M., Haddix, M. L., Paul, E. A., Plante, A. F., & Six, J. (2008b). Experimental warming shows that decomposition temperature sensitivity increases with soil organic matter recalcitrance. *Ecology, 89*(9), 2384-2391. https://doi.org/10.1890/08-0137.1

Craine, J. M., Fierer, N., & McLauchlan, K. K. (2010). Widespread coupling between the rate and temperature sensitivity of organic matter decay. *Nature Geoscience, 3*(12), 854-857. https://doi.org/10.1038/ngeo1009

Crowther, T., Todd-Brown, K., Rowe, C., Wieder, W., Carey, J., Machmuller, M., Bradford, M. (2016). Quantifying global soil carbon losses in response to warming. *Nature, 540*(7631), 104-108. https://doi.org/10.1038/nature20150

Davidson, E. A., & Janssens, I. A. (2006). Temperature sensitivity of soil carbon decomposition and feedbacks to climate change. *Nature, 440*(7081), 165-173. https://doi.org/10.1038/nature04514

Davidson, E. A., Janssens, I. A., & Luo, Y. (2006). On the variability of respiration in terrestrial ecosystems: moving beyond Q_{10}. *Global Change Biology, 12*(2), 154-164. https://doi.org/10.1111/j.1365-2486.2005.01065.x

Davidson, E. A., Samanta, S., Caramori, S. S., & Savage, K. (2012). The Dual Arrhenius and

Michaelis–Menten kinetics model for decomposition of soil organic matter at hourly to seasonal time scales. *Global Change Biology, 18*(1), 371-384. https://doi.org/10.1111/j.1365-2486.2011.02546.x

Ding, F., Sun, W., Huang, Y., & Hu, X. (2018). Larger Q_{10} of carbon decomposition in finer soil particles does not bring long-lasting dependence of Q_{10} on soil texture. *European Journal of Soil Science, 69*(2), 336-347. https://doi.org/10.1111/ejss.12530

Dungait, J. A. J., Hopkins, D. W., Gregory, A. S., & Whitmore, A. P. (2012). Soil organic matter turnover is governed by accessibility not recalcitrance. *Global Change Biology*, *18*(6), 1781-1796. https://doi.org/10.1111/j.1365-2486.2012.02665.x

Fang, C. M., Smith, P., Moncrieff, J. B., & Smith, J. U. (2005). Similar response of labile and resistant soil organic matter pools to changes in temperature. *Nature, 433*(7021), 57-59. https://doi.org/10.1038/nature03138

Gentsch, N., Wild, B., Mikutta, R., Čapek, P., Diáková, K., Schrumpf, M., . . . Guggenberger, G. (2018). Temperature response of permafrost soil carbon is attenuated by mineral protection. *Global Change Biology, 24*(8), 3401-3415. https://doi.org/10.1111/gcb.14316

Gershenson, A., Bader, N. E., & Cheng, W. (2009). Effects of substrate availability on the temperature sensitivity of soil organic matter decomposition. *Global Change Biology,15*(1), 176-183. https://doi.org/10.1111/j.1365-2486.2008.01827.x

Giardina, C. P., & Ryan, M. G. (2000). Evidence that decomposition rates of organic carbon in mineral soil do not vary with temperature. *Nature, 404*(6780), 858-861. https://doi.org/10.1038/35009076

Gillabel, J., Cebrian-Lopez, B., Six, J., & Merckx, R. (2010). Experimental evidence for the attenuating effect of SOM protection on temperature sensitivity of SOM decomposition. *Global Change Biology, 16*(10), 2789-2798. https://doi.org/10.1111/j.1365-2486.2009.02132.x

Guo, Z. T., Ruddiman, W. F., Hao, Q. Z., Wu, H. B., Qiao, Y. S., Zhu, R. X., . . . Liu, T. S. (2002). Onset of Asian desertification by 22 Myr ago inferred from loess deposits in China. *Nature, 416*(6877), 159-163. https://doi.org/10.1038/416159a

Hassink, J., & Whitmore, A. P. (1997). A model of the physical protection of organic matter in soils. *Soil Science Society of America Journal, 61*(1), 131-139. https://doi.org/10.2136/sssaj1997.03615995006100010020x

Hicks Pries, C. E., Castanha, C., Porras, R. C., & Torn, M. S. (2017). The whole-soil carbon flux in response to warming. *Science, 355*(6332), 1420-1423. https://doi.org/10.1126/science.aal1319

IPCC. (2013). *Climate Change 2013: The Physical Science Basis: Contribution of Working Group Ⅰ to Fifth Assessment Report of the Intergovernmental Panel on Climate Change.* (T. F. Stocker, D. Qin, G. K. Plattner, M. Tignor, S. K. Allen, J. Boschung, A. Nauels, Y. Xia, V. Bex, & P. M. Midgley Eds.). Cambridge, United Kingdom and New York, NY, USA: Cambridge University Press.

Jia, Y., Kuzyakov, Y., Wang, G., Tan, W., Zhu, B., & Feng, X. (2020). Temperature sensitivity of decomposition of soil organic matter fractions increases with their turnover time. *Land Degradation and Development*, *31*(5), 632-645. https://doi.org/10.1002/ldr.3477

Jin, H., Su, Z., Sun, L., Sun, Z., Hong, Z., & Jin, L. (2004). Holocene climatic change in Hunshandake Desert. *Chinese Science Bulletin, 49*(16), 1730-1735. https://doi.org/10.1007/BF03184307

Jobbagy, E. G., & Jackson, R. B. (2000). The vertical distribution of soil organic carbon and its relation to climate and vegetation. *Ecological Applications*. *10*(2), 423-436, https://doi.org/10.2307/2641104

Kaiser, K., & Guggenberger, G. (2003). Mineral surfaces and soil organic matter. *European Journal of Soil Science*, *54*(2), 219-236, https://doi.org/10.1046/j.1365-2389.2003.00544.x

Karhu, K., Auffret, M. D., Dungait, J. A., Hopkins, D. W., Prosser, J. I., Singh, B. K., Hartley, I. P. (2014). Temperature sensitivity of soil respiration rates enhanced by microbial community response. *Nature, 513*(7516), 81-84. https://doi.org/10.1038/nature13604

Knorr, W., Prentice, I. C., House, J. I., & Holland, E. A. (2005). Long-term sensitivity of soil carbon turnover to warming. *Nature, 433*(7023), 298-301. https://doi.org/10.1038/nature03226

Kuzyakov Y., Jones D.L. (2006). Glucose uptake by maize roots and its transformation in the rhizosphere. *Soil Biology and Biochemistry*, *38*(5), 851-860. https://doi.org/10.1016/j.soilbio.2005.07.012

Lai, J., Zou, Y., Zhang, J., & Peres-Neto, P. R. (2022). Generalizing hierarchical and variation partitioning in multiple regression and canonical analyses using the rdacca.hp R package. *Methods in Ecology and Evolution*. *00*, 1-7. https://doi.org/10.1111/2041-210x.13800

Lavallee, J., Soong, J., & Cotrufo, M. F. (2020). Conceptualizing soil organic matter into particulate and mineral-associated forms to address global change in the 21st century. *Global Change Biology*, *26*(1), 261-273. http://doi.org/10.1111/gcb.14859

Li, H., Yang, S., Semenov, M. V., Yao, F., Ye, J., Bu, R., Kuzyakov, Y. (2021). Temperature sensitivity of SOM decomposition is linked with a K-selected microbial community. *Global Change Biology, 27*(12), 2763-2779. https://doi.org/10.1111/gcb.15593

Li, J., Yan, D., Pendall, E., Pei, J., Noh, N. J., He, J. S., Fang, C. (2018). Depth dependence of soil carbon temperature sensitivity across Tibetan permafrost regions. *Soil Biology and Biochemistry, 126*, 82-90. https://doi.org/10.1016/j.soilbio.2018.08.015

Li, J., Zhang, Q., Li, Y., Liu, Y., Xu, J., & Di, H. (2017). Effects of long-term mowing on the fractions and chemical composition of soil organic matter in a semiarid grassland. *Biogeosciences, 14*(10), 2685-2696. https://doi.org/10.5194/bg-14-2685-2017

Li, X., Xie, J., Zhang, Q., Lyu, M., Xiong, X., Liu, X., Yang, Y. (2020). Substrate availability and soil microbes drive temperature sensitivity of soil organic carbon mineralization to warming along an elevation gradient in subtropical Asia. *Geoderma, 364*, 114198. https://doi.org/10.1016/j.geoderma.2020.114198

Li, Y., Jiang, P., Chang, S. X., Wu, J., & Lin, L. (2010). Organic mulch and fertilization affect soil carbon pools and forms under intensively managed bamboo (Phyllostachys praecox) forests in southeast China. *Journal of Soils and Sediments, 10*(4), 739-747. https://doi.org/10.1007/s11368-010-0188-4

Lindsay, W. L. (1978). Development of a DTPA soil test for zinc, iron, manganese, and copper. *Soil Science Society of America Journal, 42*(3), 421-428.

https://doi.org/10.2136/sssaj1978.03615995004200030009x

Liu C, Tian H, Gu X, Li N, Zhao X, Lei M, Alharbi H, Megharaj M, He W, Kuzyakov Y (2022). Catalytic efficiency of soil enzymes explains temperature sensitivity: insights from physiological theory. *Science of the Total Environment*, *822*, 153365. https://doi.org/10.1016/j.scitotenv.2022.153365

Liu, Y., Wang, C., He, N., Wen, X., Gao, Y., Li, S., . . . Yu, G. (2017). A global synthesis of the rate and temperature sensitivity of soil nitrogen mineralization: latitudinal patterns and mechanisms. *Global Change Biology, 23*(1), 455-464. https://doi.org/10.1111/gcb.13372

Liu, Y., Xu, L., Zheng, S., Chen, Z., Cao, Y., Wen, X., & He, N. (2021). Temperature sensitivity of soil microbial respiration in soils with lower substrate availability is enhanced more by labile carbon input. *Soil Biology and Biochemistry*, *154*, 108148. https://doi.org/10.1016/j.soilbio.2021.108148

Loeppmann, S., Blagodatskaya, E., Pausch, J., & Kuzyakov, Y. (2016). Enzyme properties down the soil profile – A matter of substrate quality in rhizosphere and detritusphere. *Soil Biology and Biochemistry*, *103*, 274-283. https://doi.org/10.1016/j.soilbio.2016.08.023

Lugato, E., Lavallee, J., Haddix, M., Panagos, P., & Cotrufo, M. F. (2021). Different climate sensitivity of particulate and mineral-associated soil organic matter. *Nature Geoscience*, *14*(5), 295-300. https://doi.org/10.1038/s41561-021-00744-x

Luo, Z., Wang, G., & Wang, E. (2019). Global subsoil organic carbon turnover times dominantly controlled by soil properties rather than climate. *Nature Communications, 10*(1), 3688. https://doi.org/10.1038/s41467-019-11597-9

Maharjan M., Sanaullah M., Razavi B.S., Kuzyakov Y. (2017). Effect of land use and management practices on microbial biomass and enzyme activities in subtropical top- and sub-soils. *Applied Soil Ecology*, *113*, 22-28. http://dx.doi.org/10.1016/j.apsoil.2017.01.008

Márquez, C. O., Garcia, V. J., Cambardella, C. A., Schultz, R. C., & Isenhart, T. M. (2004). Aggregate-size stability distribution and soil stability. *Soil Science Society of America Journal, 68*(3), 725-735. https://doi.org/10.2136/sssaj2004.7250

Metcalf, L., & Casey, W. (2016). Introduction to data analysis. In L. Metcalf & W. Casey (Eds.),

Cybersecurity and Applied Mathematics (pp. 43-65). Boston: Syngress Press.

Mikutta, R., Kleber, M., Torn, M. S., & Jahn, R. (2006). Stabilization of soil organic matter: Association with minerals or chemical recalcitrance? *Biogeochemistry, 77*(1), 25-56. https://doi.org/10.1007/s10533-005-0712-6

Ochoa-Hueso, R., Bell, M. D., & Manrique, E. (2014). Impacts of increased nitrogen deposition and altered precipitation regimes on soil fertility and functioning in semiarid Mediterranean shrublands. *Journal of Arid Environments, 104*, 106-115. https://doi.org/10.1016/j.jaridenv.2014.01.020

Pang, X., Zhu, B., Lu, X., & Cheng, W. (2015). Labile substrate availability controls temperature sensitivity of organic carbon decomposition at different soil depths. *Biogeochemistry,126*(1), 85-98. https://doi.org/10.1007/s10533-015-0141-0

Qin, S., Chen, L., Fang, K., Zhang, Q., Wang, J., Liu, F., . . . Yang, Y. (2019). Temperature sensitivity of SOM decomposition governed by aggregate protection and microbial communities. *Science Advances, 5*(7), eaau1218. https://doi.org/10.1126/sciadv.aau1218

Qin, S., Kou, D., Mao, C., Chen, Y., Chen, L., & Yang, Y. (2021). Temperature sensitivity of permafrost carbon release mediated by mineral and microbial properties. *Science Advances, 7*(32), eabe3596. https://doi.org/10.1126/sciadv.abe3596

Retallack, G. J. (2001). Alternation of palsosols after burial. In Retallack, G. J (Eds.), *Soils of the past: an introduction to paleopedology* (pp. 87-101). New York: John Wiley & Sons Press.

Schlesinger, W. H., & Andrews, J. A. (2000). Soil respiration and the global carbon cycle. *Biogeochemistry, 48*(1), 7-20. https://doi.org/10.1023/A:1006247623877

Schulten, H. R., & Leinweber, P. (2000). New insights into organic-mineral particles: composition, properties and models of molecular structure. *Biology and Fertility of Soils*, *30*(5), 399-432. https://doi.org/10.1007/s003740050020

Sheng, H., Zhou, P., Zhang, Y., Kuzyakov, Y., Zhou, Q., Ge, T., & Wang, C. (2015). Loss of labile organic carbon from subsoil due to land-use changes in subtropical China. *Soil Biology and Biochemistry*, *88*, 148-157. https://doi.org/10.1016/j.soilbio.2015.05.015

Six, J., Conant, R. T., Paul, E. A., & Paustian, K. (2002). Stabilization mechanisms of soil organic

matter: Implications for C-saturation of soils. *Plant and Soil, 241*(2), 155-176. https://doi.org/10.1023/A:1016125726789

Six, J., Elliott, E. T., Paustian, K., & Doran, J. W. (1998). Aggregation and soil organic matter accumulation in cultivated and native grassland soils. *Soil Science Society of America Journal, 62*(5), 1367-1377. https://doi.org/10.2136/sssaj1998.03615995006200050032x

Smith, P., & Fang, C. (2010). Carbon cycle: A warm response by soils. *Nature, 464*(7288), 499-500. https://doi.org/10.1038/464499a

Sollins, P., Homann, P., & Caldwell, B. A. (1996). Stabilization and destabilization of soil organic matter: mechanisms and controls. *Geoderma*, *74*(1), 65-105. https://doi.org/10.1016/S0016-7061(96)00036-5

Tang, J., Cheng, H., & Fang, C. (2017). The temperature sensitivity of soil organic carbon decomposition is not related to labile and recalcitrant carbon. *PLoS One, 12*(11), e0186675. https://doi.org/10.1371/journal.pone.0186675

Tarnocai, C., Canadell, J. G., Schuur, E. A. G., Kuhry, P., Mazhitova, G., & Zimov, S. (2009). Soil organic carbon pools in the northern circumpolar permafrost region. *Global Biogeochemical Cycles, 23*(2), GB2023. https://doi.org/10.1029/2008gb003327

Thiessen, S., Gleixner, G., Wutzler, T., & Reichstein, M. (2013). Both priming and temperature sensitivity of soil organic matter decomposition depend on microbial biomass – An incubation study. *Soil Biology and Biochemistry*, *57*, 739-748. https://doi.org/10.1016/j.soilbio.2012.10.029

Todd-Brown, K. E. O., Randerson, J. T., Hopkins, F., Arora, V., Hajima, T., Jones, C., . . . Allison, S. D. (2014). Changes in soil organic carbon storage predicted by Earth system models during the 21st century. *Biogeosciences, 11*(8), 2341-2356. https://doi.org/10.5194/bg-11-2341-2014

Trumbore, S. E., & Czimczik, C. I. (2008). An uncertain future for soil carbon. *Science, 321*(5895), 1455-1456. https://doi.org/10.1126/science.1160232

van Steenbergen, M., Cambardella, C. A., Elliott, E. T., & Merckx, R. (1991). Two simple indexes for distribution of soil components among size classes. *Agriculture, Ecosystems and*

Environment, 34(1), 335-340. https://doi.org/10.1016/0167-8809(91)90119-I

Vance, E. D., Brookes, P. C., & Jenkinson, D. S. (1987). An extraction method for measuring soil microbial biomass C. *Soil Biology and Biochemistry, 19*(6), 703-707. https://doi.org/10.1016/0038-0717(87)90052-6

von Lützow, M., & Kögel-Knabner, I. (2009). Temperature sensitivity of soil organic matter decomposition – what do we know? *Biology and Fertility of Soils*, *46*(1), 1-15. https://doi.org/10.1007/s00374-009-0413-8

Wang, C., Morrissey, E. M., Mau, R. L., Hayer, M., Piñeiro, J., Mack, M. C., . . . Hungate, B. A. (2021). The temperature sensitivity of soil: microbial biodiversity, growth, and carbon mineralization. *The ISME Journal*, *15*(9), 2738–2747. https://doi.org/10.1038/s41396-021-00959-1

Wang, Q., He, N., Yu, G., Gao, Y., Wen, X., Wang, R., . . . Yu, Q. (2016). Soil microbial respiration rate and temperature sensitivity along a north-south forest transect in eastern China: Patterns and influencing factors. *Journal of Geophysical Research: Biogeosciences,121*(2), 399-410. https://doi.org/10.1002/2015jg003217

Wang, Q., Liu, S., & Tian, P. (2018). Carbon quality and soil microbial property control the latitudinal pattern in temperature sensitivity of soil microbial respiration across Chinese forest ecosystems. *Global Change Biology, 24*(7), 2841-2849. https://doi.org/10.1111/gcb.14105

Wang, Y., Hu, N., Ge, T., Kuzyakov, Y., Wang, Z. L., Li, Z., ... Lou, Y. (2017). Soil aggregation regulates distributions of carbon, microbial community and enzyme activities after 23-year manure amendment. *Applied Soil Ecology*, *111*, 65-72. https://doi.org/10.1016/j.apsoil.2016.11.015

Wang, Y., Wang, Z. L., Zhang, Q., Hu, N., Li, Z., Lou, Y., ... Kuzyakov, Y. (2018). Long-term effects of nitrogen fertilization on aggregation and localization of carbon, nitrogen and microbial activities in soil. *Science of the Total Environment*, *624*, 1131-1139. https://doi.org/10.1016/j.scitotenv.2017.12.113

West, A. W., & Sparling, G. P. (1986). Modifications to the substrate-induced respiration method

to permit measurement of microbial biomass in soils of differing water contents. *Journal of Microbiological Methods*, *5*(3), 177-189. https://doi.org/10.1016/0167-7012(86)90012-6

Xu, X., Yang, B., Wang, H., Cao, Y., Li, K., & Gao, S. (2019). Temperature sensitivity of soil heterotrophic respiration is altered by carbon substrate along the development of Quercus Mongolica forest in northeast China. *Applied Soil Ecology, 133*, 52-61. https://doi.org/10.1016/j.apsoil.2018.09.010

Zamanian, K., Pustovoytov, K., & Kuzyakov, Y. (2016). Pedogenic carbonates: Forms and formation processes. *Earth-Science Reviews, 157*, 1-17. https://doi.org/10.1016/j.earscirev.2016.03.003

Zimmermann, M., Leifeld, J., Conen, F., Bird, M. I., & Meir, P. (2010). Can composition and physical protection of soil organic matter explain soil respiration temperature sensitivity? *Biogeochemistry*, *107*(1), 423-436. https://doi.org/10.1007/s10533-010-9562-y

Zhou, L. P., Oldfield, F., Wintle, A. G., Robinson, S. G., & Wang, J. T. (1990). Partly pedogenic origin of magnetic variations in Chinese loess. *Nature, 346*(6286), 737-739. https://doi.org/10.1038/346737a0

Zhu, B., & Cheng, W. (2011). Rhizosphere priming effect increases the temperature sensitivity of soil organic matter decomposition. *Global Change Biology, 17*(6), 2172-2183. https://doi.org/10.1111/j.1365-2486.2010.02354.x

Figures:

Fig. 1. Logical workflow diagram of the experimental procedure.

Fig. 2. Heuristic example of temperature sensitivity (Q_{10}) following the Michaelis–Menten kinetics. Q_{10} of the V_{max} was assigned a value of 2 in all four scenarios, and the substrateavailability [S] was assumed temperature independent (it did not change with temperature). For the Q_{10} of K_m we considered values of 2 (see the red line) or 1.5 (see the blue line). The K_m at low temperatures was set to a low value (1; see the solid line) and a high value (10; see the dashed line). P_1, P_i and P_2 represent the point of maximum acceleration of Q_{10} increase, the inflexion point (P_i, corresponding to a null acceleration of Q_{10}), and the maximum negative acceleration of the sigmoid curve, respectively. Values of [S] are in arbitrary units.

Fig. 3. Changes of SOM chemical complexity and physical protection and mineral association with soil age. (a) Solid-state ^{13}C-NMR spectra of paleosol organic matter for seven paleosol layers, all spectra were separated into seven groups. (b) Relationship between A/O-A (alkyl C to O-alkyl C ratio) and soil age. The A/O-A index, increased with SOM chemical complexity, represents the extent of SOM decomposition (c) Relationship between GMD (geometric mean diameter) and soil age. (d) The proportion of C in POM and MAOM. The linear regression lines with 95% confidence intervals reflect the predicted effects of fixed factors. All regression lines are significant at $p < 0.001$.

Fig. 4. The relationship between soil age, carbon availability and Q_{10} and the relative importance of five edaphic factors on Q_{10}. (a) Q_{10} changes along the Holocene paleosol chronosequence. The asterisks indicate significant differences in the Q_{10} values between S0 (500 a BP) and S1–S6 (from 1,150 to 6,900 a BP) ($p < 0.0001$). (b) Correlation matrix between five grouped variables. (c) Relative importance of five multivariate functional indices on Q_{10}. (d) The relationship between C availability and Q_{10}, values of C availability index is in arbitrary units. CEC is the cation exchangeable capacity. AOA is the ratio of alkyl C to O-alkyl C. The linear regression lines with

95% confidence intervals reflect the predicted effects of fixed factors. All regression lines are significant at $p < 0.0001$.

Fig. 5. Changes of temperature sensitivity in three incubation experiments (see Exp2 - 4 in Methods). (a) Q_{10} values in soils along the chronosequence with or without inocula (Exp2). The asterisks indicate significant differences in the Q_{10} values between S0 (500 a BP) and S1–S6 (from 1,150 to 6,900 a BP) ($p < 0.0001$). (b) Changes of Q_{10} with incubation time (Exp4). (c) Q_{10} values with and without glucose addition. (d) Q_{10} of ^{13}C-labelled glucose ($Q_{10}^{glucose}$) depending on soil age (Exp3). Given the non-normally distributed data, the non-parametric test (the Kruskal–Wallis test) was used to detect the significant difference of $Q_{0}^{glucose}$ values. The letters indicate the results of the two-way ANOVA. The linear regression lines with 95% confidence intervals reflect the predicted effects of fixed factors. The regression line in (d) is significant at $p < 0.0001$ for S0 (500 a BP), and insignificant at $p > 0.05$ for S1 to S6 (except for S5, which significant at $p < 0.05$).

Fig. 6. Conceptual diagrams of carbon (C) availability and quality controls on temperature sensitivity of SOM decomposition. Q_{10} was logistically and exponentially increased with log-transformed substrate availability [S] and activation energy (E_a) in theoretical simulation (a,b). (c) Q_{10} was nonlinearly increased with the C availability index in paleosols, which coincide well with our simulation in (a) (the red solid line represents the theoretical stimulation of Q_{10} with increase of [S], seven blue dots represent Q_{10} values in S0 to S6, and the yellow dot was the average Q_{10} values of all paleosols when C limitation was released after glucose addition). (d) Q_{10} was exponentially increased with activation energy (E_a) in S0 which is in line with theoretical simulation in (b), suggesting C quality decreased due to the depletion of labile C with the duration of incubation. Red dots represent the Q_{10} on day 1, 4, 10, 24, respectively. Regression line in (d) is significantly increasing at $p < 0.0001$, which is well explained by Arrhenius equation.

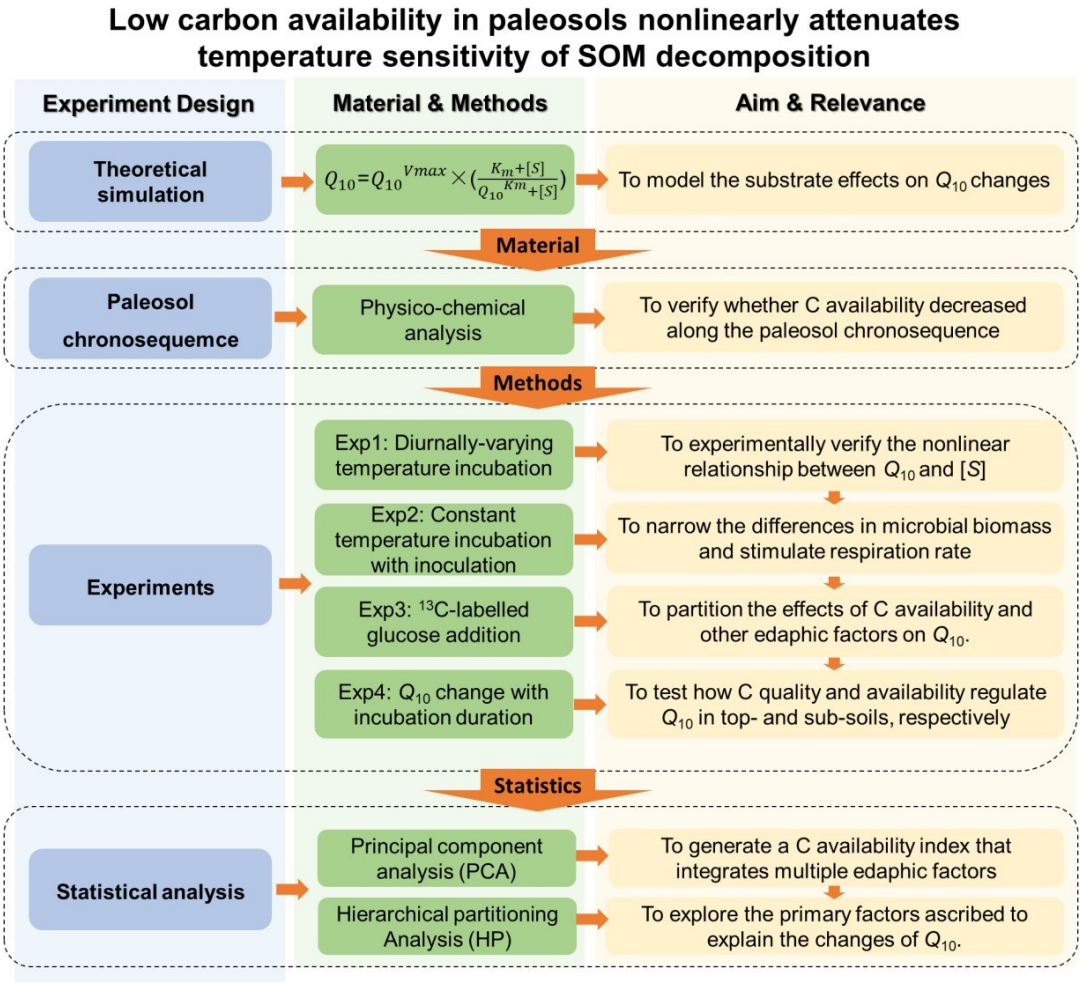

Fig. 1.

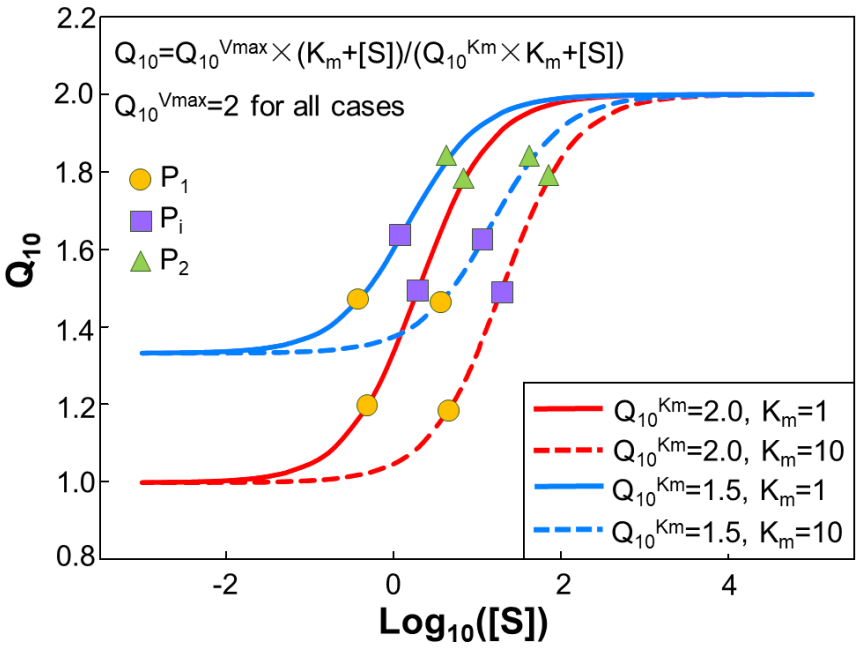

Fig. 2.

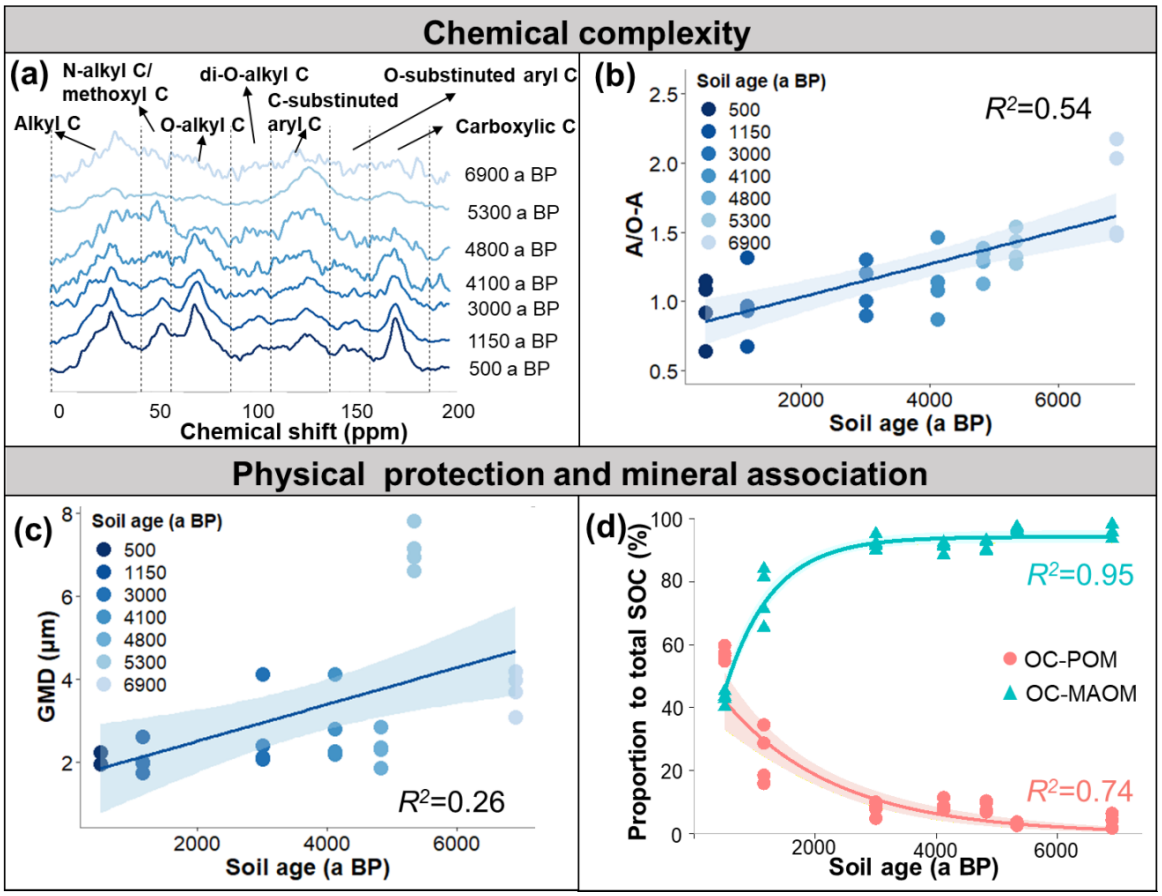

Fig. 3.

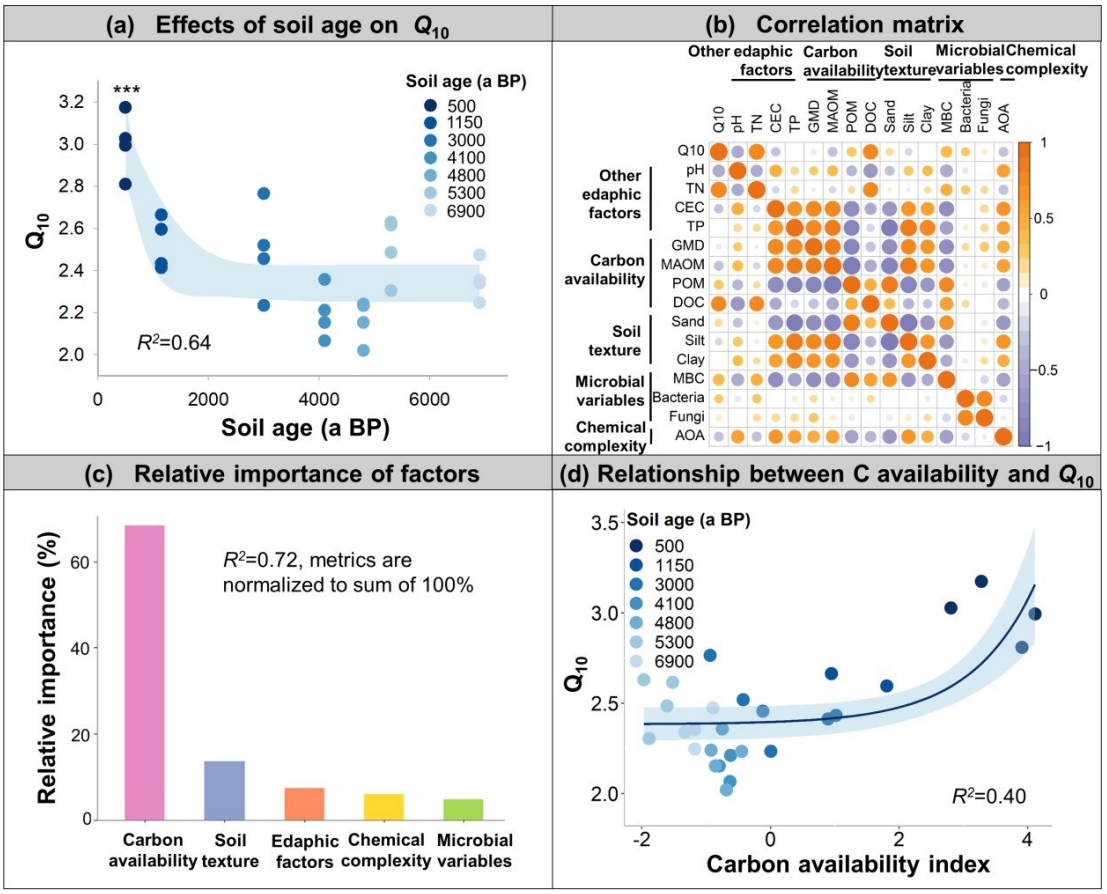

Fig. 4.

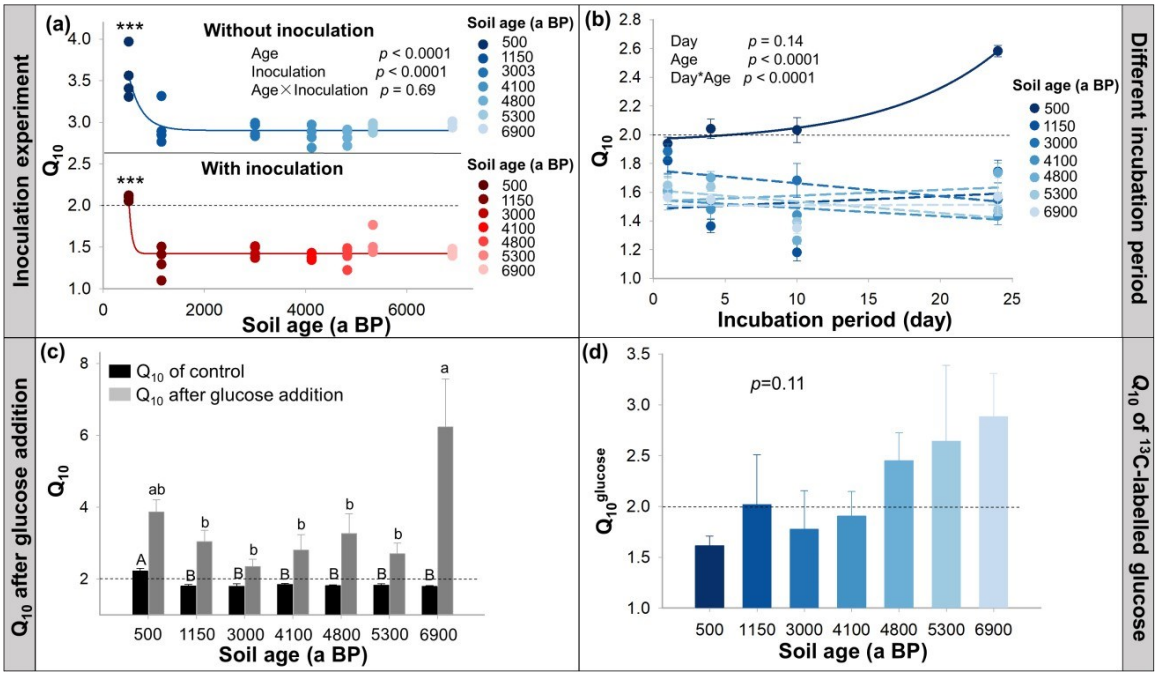

Fig. 5.

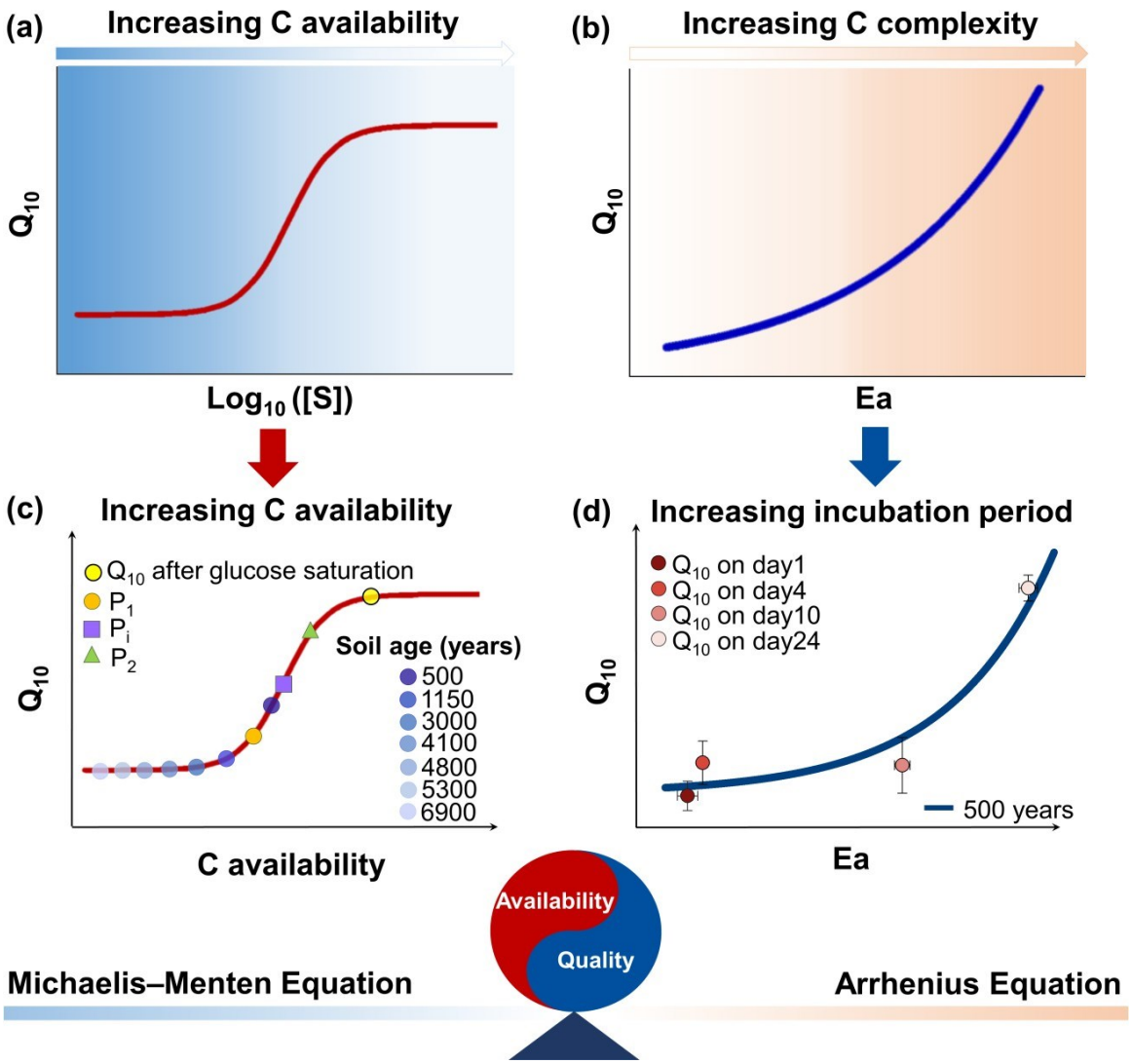

Fig. 6.